

# Feasibility study on a novel tiny dosimeter using a barium titanate capacitor

Yuma Kuga<sup>1</sup>, Ryo Ogawara<sup>2</sup> and Masayori Ishikawa<sup>3,\*</sup>

<sup>1</sup>Graduate School of Biomedical Science and Engineering, Hokkaido University, N-15 W-7 Kita-ku, Sapporo Hokkaido, 060-8638, Japan

<sup>2</sup>National Institute of Radiological Sciences, National Institutes for Quantum and Radiological Science and Technology, 4-9-1 Anagawa, Inage-ku, Chiba-shi, Chiba, 263-8555, Japan

<sup>3</sup>Graduate School of Health Sciences, Hokkaido University, N-12 W-5 Kita-ku, Sapporo Hokkaido, 060-0812, Japan

\*Corresponding author: Masayori Ishikawa, Affiliation: Graduate School of Health Sciences, Hokkaido University, Full postal address: N-12 W-5 Kita-ku, Sapporo Hokkaido, 060-0812, Japan, E-mail: masayori@med.hokudai.ac.jp, Tel: +81-11-706-3411, Fax: +81-11-706-3192

(Received 23 May 2019; revised 25 June 2019; editorial decision 2 November 2019)

## ABSTRACT

In our laboratory we have confirmed that the capacitance of barium titanate-based capacitors changes due to radiation. Since a commercially available capacitor is very small and inexpensive, it may be used as a multidimensional dose meter in which a large number of capacitor elements are arranged, or may be embedded in the body and used as an in-vivo dose meter. In this study we examined the usefulness of a dosimeter using the capacitance change of a barium titanate capacitor. As a basic property, it was confirmed that the dose linearity was good. With regard to dose rate characteristics and response to fractionated irradiation, capacitance change due to aging affects measurement accuracy, but online measurement of capacitance change immediately before irradiation can be performed to correct aging effects during irradiation. By doing this, we confirmed that the dose rate characteristics and the response to fractionated radiation are improved.

**Keywords:** Barium Titanate capacitor; tiny dosimeter; in-vivo dosimeter; array dosimeter

## INTRODUCTION

Radiation therapy is one of several cancer treatment methods. It has less physical burden than surgical treatment, and the disease can be treated while preserving healthy function and form. Because high-precision radiation therapy requires that the tumor be given a sufficient dose while suppressing the dose to organs at risk, intensity modulated radiation treatment (IMRT) is often performed [1]. Due to the complexity of dose delivery with highly modulated radiation, dose distribution measurements are performed in advance to confirm the dose delivered to each patient [2]. Films are generally used for dose distribution measurements, but in recent years multidimensional dosimeters in which ionization chambers and semiconductor detectors are arranged in two or three dimensions have also been used [3]. Multidimensional dosimeters have the advantage of being able to measure in real time, but they are inferior to films in terms of spatial resolution [4]. In order to improve the spatial resolution, it is necessary to arrange more detector elements, but this is not realistic because the unit price of the elements is too high, resulting in a very expensive dosimeter. On the other hand, the capacitor is one of the important electronic circuits, and according to the previous research, it has been confirmed

that the characteristics change by irradiation with radiation [5]. In addition, there have been several prior studies on dosimeters using capacitance changes of capacitors, and many have used MOSFETs [6, 7]. We found that the capacitance changes when radiation is applied to a multilayer ceramic capacitor using barium titanate. In addition, since capacitors are relatively inexpensive, by arranging a large number of capacitors, it is possible to construct an inexpensive, high-resolution multi-dimensional dose meter.

In addition, since the barium titanate capacitor is very small (minimum  $0.4 \times 0.2 \times 0.2 \text{ mm}^3$ ), it may be used in the vicinity of a tumor to be used as an *in-vivo* dosimeter. This paper reports basic characteristics (dose linearity and dose rate dependency) in order to use a barium titanate capacitor as a dosimeter. At present, the relationship between crystal structure change and capacitance change of barium titanate due to irradiation is not clear. In previous studies, irradiation experiments were conducted on calcium titanate, which has the same crystal structure as barium titanate, but the same relationship is not described. For this reason, the mechanism of capacitance change due to irradiation is out of the scope of this paper and is therefore omitted.

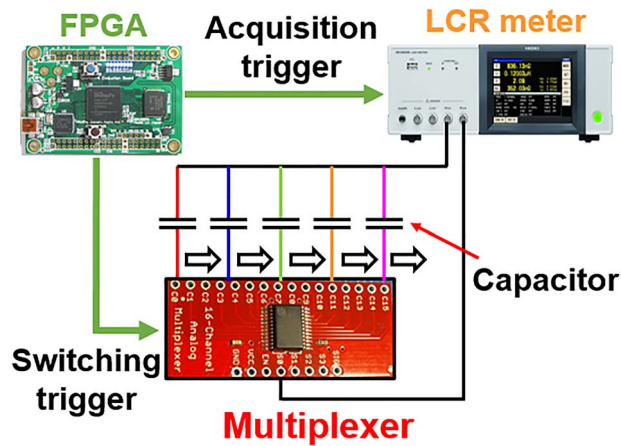


Fig. 1. Capacitance Measurement System.

## MATERIALS & METHODS

### Barium titanate multilayer ceramic capacitor

Various dielectrics are used for multilayer ceramic capacitors according to their individual properties. However, since only a capacitor with barium titanate as a dielectric causes a capacitance change by radiation irradiation, a multilayer ceramic capacitor chip (GCM188R72A223KA01) manufactured by Murata Manufacturing was used in this research. The physical density of the barium titanate is  $6.152 \text{ g/cm}^3$  and the shape of the capacitor is  $0.8 \text{ mm}$  square and the length is  $1.6 \text{ mm}$ .

### Capacitance measurement system

In order to conduct a basic study of the dosimeter, it was necessary to measure the capacitance change of the capacitor. An LCR meter (IM 3536 manufactured by HIOKI) was used for the measurement. Moreover, since the measurement object develops high impedance, it was measured by the two-terminal method. Since the LCR meter can only read a single capacitor, we built a system that can measure the capacitance of five capacitors using a field programmable gate array (FPGA) and an analog multiplexer (Fig. 1). The capacitance change of one capacitor element was measured every 12 seconds.

### Experiment system

Figure 2 shows the experimental system and the details of the capacitors used. A medical high energy X-ray treatment apparatus (Clinac 6EX manufactured by Varian Medical Systems) installed at Hokkaido University Radioisotope Center was used. The irradiation field was set to  $10 \text{ cm} \times 10 \text{ cm}$  and a solid water phantom (manufactured by Kyoto Kagaku, Tough Water) was used. The source to surface distance (SSD) was  $100 \text{ cm}$ . In addition, the source to target distance (STD) was fixed at  $101.5 \text{ cm}$ . The maximum dose rate depth was used. A solid water phantom of  $10 \text{ cm}$  was installed on the lower side of the capacitor to consider backscattering effects. Measurement was carried out by burying five capacitors in a heat-resistant epoxy resin to reduce side scattering around the capacitors and annealing treatment at high temperature was conducted. For wiring to each capacitor, a seal substrate (ICB-053 manufactured by Sunhayato) in which a conductive

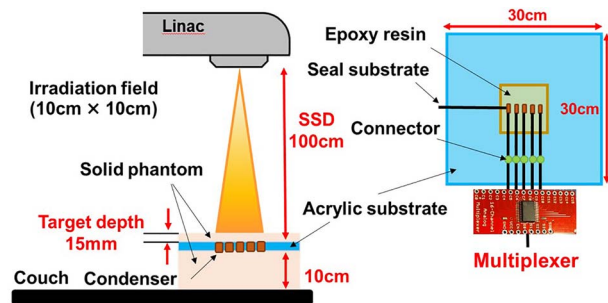


Fig. 2. Radiation system and layout of the capacitors relative to the linac.

wire is printed on a  $0.1 \text{ mm}$  thick glass epoxy substrate was used in order to minimize the influence of scattering by the metal conductive wire. After constructing the above measurement system, the following five verification experiments were conducted.

### Performance evaluation as the dosimeter

#### Change of capacitance due to X-ray irradiation

In order to confirm the capacitance change of the capacitor and the linearity of the dose, five sets of multilayer ceramic capacitors were irradiated with doses of 5, 10, 20, 50 and  $100 \text{ Gy}$  at  $600 \text{ cGy/min}$ . The relationship between the radiation dose and the capacitance change was then examined.

#### Dose-rate dependence

In order to evaluate the dose rate dependency of the capacitance change,  $10 \text{ Gy}$  was irradiated to each of the five multilayer ceramic capacitor sets at a dose-rate of 100, 200, 400,  $600 \text{ cGy/min}$ . The variation in capacitance change was then calculated.

#### Capacitance change with fractionated X-ray irradiation

In radiotherapy, fractionated irradiation is generally performed, and it is necessary to compare the difference in capacitance change between single irradiation and fractionated irradiation. Capacitance change was therefore measured by irradiating the five multilayer ceramic capacitors with five patterns of  $50 \text{ Gy} \times 1$ ,  $25 \text{ Gy} \times 2$ ,  $12.5 \text{ Gy} \times 4$ ,  $10 \text{ Gy} \times 5$  and  $5 \text{ Gy} \times 10$  times with dose rate at  $600 \text{ cGy/min}$ .

#### Optimization of the annealing temperature

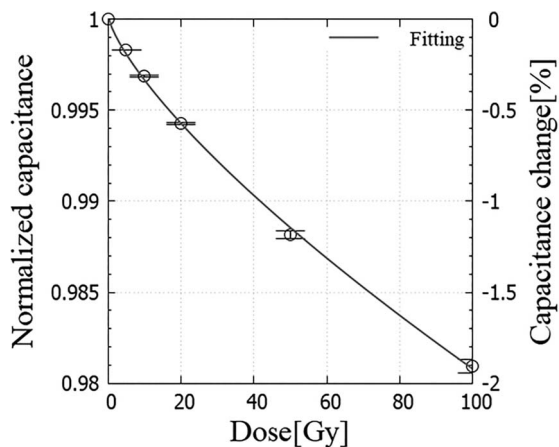
Capacitors using barium titanate are known to undergo a phenomenon (annealing) in which the crystal structure changes and the capacitance recovers upon heating above the Curie temperature. After the irradiated capacitor was annealed in an electric furnace, the capacitance change when the same dose was irradiated again was examined. In annealing, it is necessary to exceed the Curie temperature ( $127 \text{ }^\circ\text{C}$ ) which is the crystal transition temperature of barium titanate. In order to study the optimization of the annealing temperature, the annealing treatment was performed by holding for 1 hour at  $100 \text{ }^\circ\text{C}$ ,  $115 \text{ }^\circ\text{C}$ ,  $130 \text{ }^\circ\text{C}$ ,  $145 \text{ }^\circ\text{C}$  and  $160 \text{ }^\circ\text{C}$  for irradiation of  $30 \text{ Gy}$  at  $600 \text{ cGy/min}$  [8], respectively. We also examined the repeatability of capacitance change.

**Table 1. Capacitance change before and after irradiation**

(a) Capacitance before and after irradiation								
Dose[Gy]	Irradiation	Capacitance[nF]						
		No.1	No.2	No.3	No.4	No.5		
5	Before	26.454	25.836	27.102	26.707	25.554		
	After	26.409	25.792	27.056	26.661	25.510		
10	Before	26.841	26.642	25.704	26.180	25.918		
	After	26.756	26.557	25.624	26.099	25.834		
20	Before	26.809	26.378	26.799	26.692	26.290		
	After	26.656	26.227	26.645	26.542	26.138		
50	Before	26.685	26.397	25.967	25.693	25.471		
	After	26.369	26.078	25.650	25.385	25.176		
100	Before	26.078	25.930	25.869	27.189	26.834		
	After	25.570	25.427	25.384	26.685	26.322		

(b) Capacitance change according to irradiation dose								
Dose[Gy]	Normalized capacitance					Capacitance change		
	No.1	No.2	No.3	No.4	No.5	Average	Change	Relative SD
5	0.9983	0.9983	0.9983	0.9983	0.9983	0.9983	0.1710%	0.6264%
10	0.9969	0.9968	0.9969	0.9969	0.9968	0.9969	0.3146%	1.5734%
20	0.9943	0.9943	0.9943	0.9944	0.9942	0.9943	0.5722%	1.0061%
50	0.9882	0.9879	0.9878	0.9880	0.9884	0.9881	1.1933%	1.9834%
100	0.9805	0.9806	0.9812	0.9815	0.9809	0.9810	1.9041%	2.1479%



**Fig. 3. Relationship between radiation dose and capacitance change.**

**Repeatability of measurement**

In order to evaluate the repeatability of the measurements, 10 different sets of plates in which five capacitors were solidified with an epoxy resin were prepared. The variation in capacitance change when 10 Gy was irradiated under the same irradiation conditions was evaluated.

**RESULTS**

**Change of capacitance due to X-ray irradiation**

Figure 3 shows the capacitance change when exposed to 5, 10, 20, 50, and 100 Gy irradiations. It was confirmed from Fig. 3 that the capacitance change increases as the irradiation dose increases. Moreover, it was confirmed that the capacitance change depending on the irradiation dose can be fitted by a function represented by  $y = \exp(-0.000645x^{0.741})$ . Here,  $x$  and  $y$  stand for irradiated dose and normalized capacitance. By making this change into a function in advance by fitting, the irradiation dose can be determined from the capacitance change. Table 1(a) shows the capacitance before and after each irradiation, and Table 1(b) shows the average value of the capacitance change rate at the irradiation dose and its standard deviation. From Table 1(b), it can be confirmed that the inter-element variation of the capacitance change at each dose is at most only 2.15%.

**Dose-rate dependency**

Figure 4 shows the capacitance change rate when 10 Gy is irradiated at a dose rate of 100, 200, 400, 600 cGy/min. Table 2 furthermore shows the average value and the standard deviation of the capacitance change rate. From Table 2, it was confirmed that the capacitance change was from 0.3146% to 0.3895% at each dose rate, and the lower the dose rate, the higher the capacitance change. Also, the standard deviation of the dose rate was 1.87%. This may be because the capacitance change of the capacitors decreases both by irradiation and aging. Therefore, at

**Table 2. Capacitance change according to dose rate.**

Dose rate [cGy/min]	Normalized capacitance						Capacitance change	
	No.1	No.2	No.3	No.4	No.5	Average	Change	Relative SD
100	0.9961	0.9961	0.9961	0.9961	0.9961	0.9961	0.3895%	0.7112%
200	0.9968	0.9968	0.9968	0.9967	0.9967	0.9968	0.3233%	1.7177%
400	0.9968	0.9968	0.9968	0.9969	0.9968	0.9968	0.3165%	1.8665%
600	0.9969	0.9968	0.9969	0.9969	0.9968	0.9969	0.3146%	1.5734%
SD of mean							0.0359%	

**Table 3. Capacitance change according to irradiation pattern.**

Irradiation Pattern	Normalized capacitance						Capacitance change	
	No.1	No.2	No.3	No.4	No.5	Average	Change	Relative SD
50Gy × 1	0.9881	0.9881	0.9881	0.9882	0.9884	0.9882	1.1836%	1.1274%
25Gy × 2	0.9881	0.9880	0.9880	0.9881	0.9883	0.9881	1.1904%	1.0232%
12.5Gy × 4	0.9874	0.9871	0.9870	0.9873	0.9877	0.9873	1.2715%	1.9916%
10Gy × 5	0.9872	0.9871	0.9871	0.9871	0.9872	0.9871	1.2870%	0.5300%
5Gy × 10	0.9863	0.9860	0.9858	0.9872	0.9867	0.9864	1.3595%	4.1503%
SD of mean							0.0732%	

a low dose rate such as 100 cGy/min, the capacitance change due to aging cannot be ignored when computing the capacitance change due to irradiation.

### Capacitance change with fractionated X-ray irradiation

Figure 5 shows the capacitance change in each irradiation pattern, and Table 3 shows the average value and the standard deviation of the capacitance change rate for each element. In each irradiation pattern, the final capacitance change was from 1.18% to 1.36%, and the capacitance change rate tended to be slightly larger as the number of irradiations increased. In addition, the standard deviation due to the irradiation pattern was slightly larger (0.0732%). This may be because, as in the case of the dose rate dependency verification, the longer the total irradiation time, the greater the decrease in capacitance due to aging.

### Optimization of the annealing temperature

Table 4 shows the difference in capacitance change due to irradiation before and after annealing. From Table 4, the capacitance change is smaller for annealing up to 115 °C compared to before annealing. On the other hand, when the annealing is performed above the Curie temperature, the capacitance change is almost the same before and after the annealing. The capacitor can therefore be repeatedly used as a dosimeter by annealing at a temperature higher than the Curie temperature.

### Repeatability of the measurements

Table 5 shows the capacitance change with 10 Gy irradiation for 10 different capacitor sets. The average value of the standard deviations of

the capacitance change with respect to five capacitor elements of each capacitor set was 1.57%, and the standard deviation with respect to the average value of the capacitance changes of five capacitor elements was 0.0056%.

## DISCUSSION

The mechanism by which the capacitance of barium titanate changes by irradiation is not yet elucidated. However, since the capacitance is affected by the difference in crystal structure, we think that the change in the crystal structure of barium titanate due to irradiation is the cause of the change in capacitance [9]. Barium titanate has an ABO<sub>3</sub>-type perovskite structure, in which the Ti ion located at the center of the crystal is displaced in the c-axis direction, causing spontaneous polarization and exhibiting ferroelectric properties [10]. The crystal structure of barium titanate is known to change with temperature, and as temperature increases, it changes to a rhombohedral, orthorhombic, tetragonal and then cubic systems (Fig. 6) [10]. Barium titanate belongs to a tetragonal system at room temperature and exhibits ferroelectric properties by spontaneous polarization. Above the Curie temperature (127 °C), the crystal structure changes to a cubic crystal, indicating the nature of a paraelectric. The capacitance shows the highest value at the conversion point between cubic and tetragonal, but when held at room temperature, an aging phenomenon occurs in which the capacitance gradually decreases. The time change of capacitance due to aging can be expressed by equations (1.1) and (1.2) [11].

$$C(t) = C_{\infty} + C_0 e^{-\left(\frac{t}{\tau(T)}\right)^{\beta}} \quad (1.1)$$

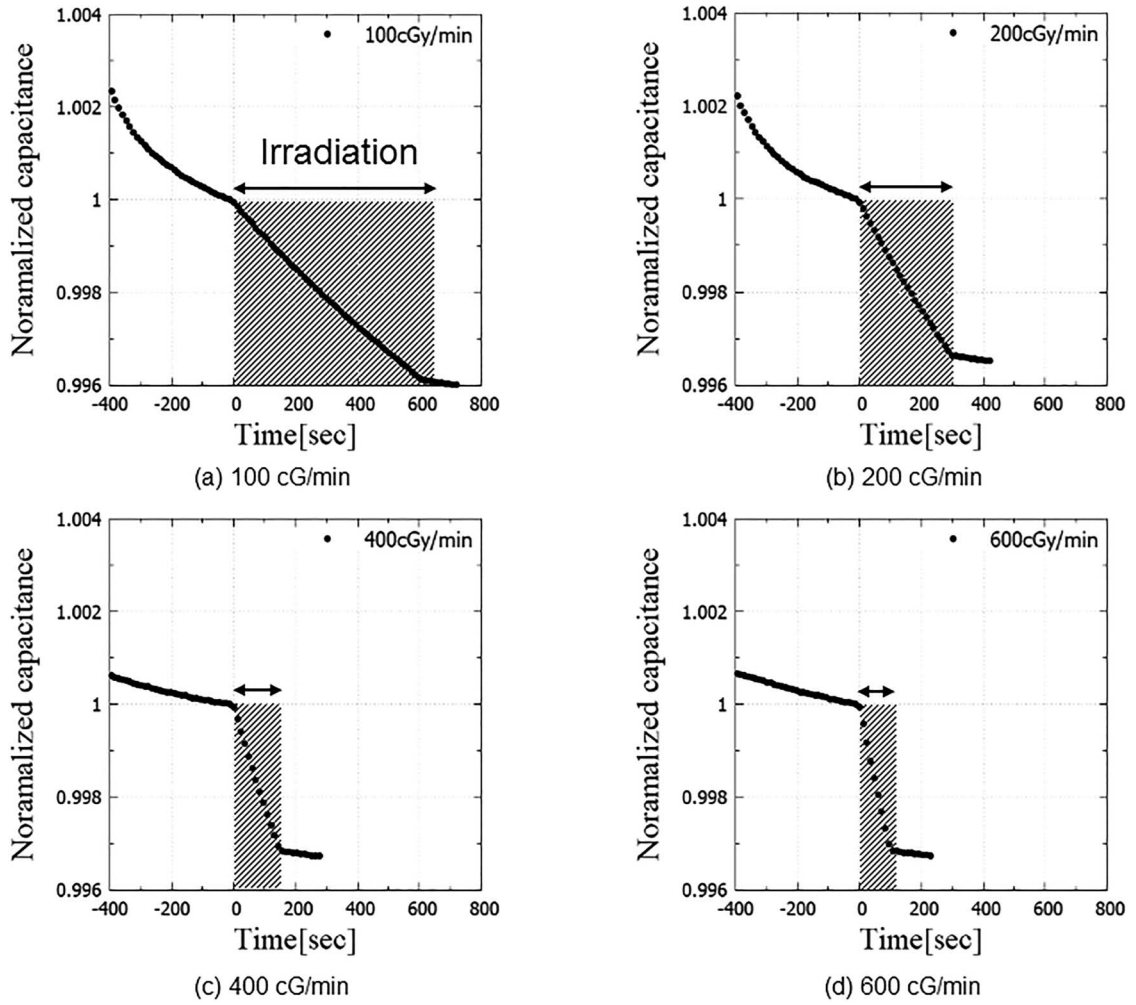


Fig. 4. Relationship between dose rate and capacitance change.

Table 4. Difference of capacitance change before and after annealing.

Temperature[°C]	Annealing	Normalized capacitance					Capacitance change		
		No.1	No.2	No.3	No.4	No.5	Average	Change	Relative SD
20 (w/o Annealing)	Before	0.9969	0.9968	0.9967	0.9968	0.9968	0.9968	0.3197%	2.1386%
	After	0.9972	0.9971	0.9971	0.9971	0.9971	0.9971	0.2854%	1.6196%
100	Before	0.9969	0.9968	0.9969	0.9968	0.9968	0.9968	0.3163%	1.0402%
	After	0.9969	0.9969	0.9969	0.9969	0.9968	0.9969	0.3138%	1.1325%
115	Before	0.9969	0.9969	0.9969	0.9970	0.9968	0.9969	0.3091%	1.8451%
	After	0.9970	0.9970	0.9970	0.9971	0.9970	0.9970	0.2994%	1.2595%
130	Before	0.9968	0.9967	0.9968	0.9968	0.9967	0.9968	0.3245%	1.2784%
	After	0.9967	0.9967	0.9968	0.9968	0.9967	0.9967	0.3253%	1.1834%
145	Before	0.9968	0.9967	0.9968	0.9968	0.9967	0.9968	0.3235%	0.8222%
	After	0.9968	0.9968	0.9969	0.9968	0.9967	0.9968	0.3188%	1.4024%
160	Before	0.9970	0.9969	0.9969	0.9969	0.9970	0.9969	0.3072%	2.0796%
	After	0.9969	0.9968	0.9968	0.9969	0.9971	0.9969	0.3090%	3.4434%

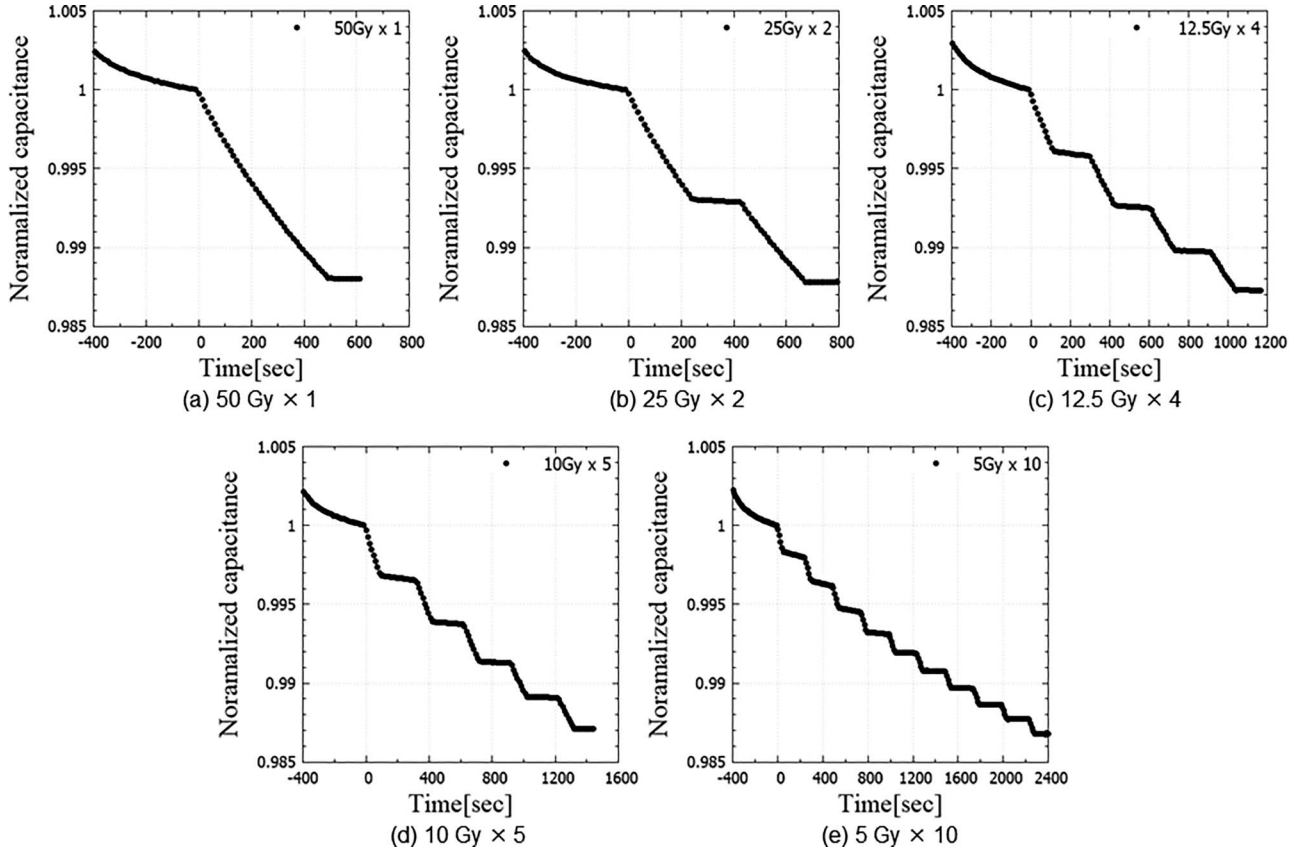


Fig. 5. Relationship between irradiation pattern and capacitance change.

Table 5. Capacitance change for 10 Gy irradiation of 10 capacitance sets.

Board Number	Normalized capacitance					Capacitance change		
	No.1	No.2	No.3	No.4	No.5	Average	Change	Relative SD
1	0.9969	0.9968	0.9968	0.9969	0.9968	0.9968	0.3163%	2.4566%
2	0.9968	0.9968	0.9968	0.9969	0.9967	0.9968	0.3190%	2.0842%
3	0.9968	0.9968	0.9968	0.9968	0.9970	0.9968	0.3153%	2.4953%
4	0.9968	0.9967	0.9968	0.9968	0.9968	0.9968	0.3210%	0.8831%
5	0.9968	0.9968	0.9968	0.9968	0.9968	0.9968	0.3213%	0.7862%
6	0.9970	0.9969	0.9969	0.9970	0.9969	0.9969	0.3057%	0.5317%
7	0.9968	0.9969	0.9970	0.9970	0.9970	0.9969	0.3053%	2.5595%
8	0.9968	0.9969	0.9969	0.9969	0.9969	0.9969	0.3132%	0.6717%
9	0.9969	0.9969	0.9969	0.9968	0.9968	0.9969	0.3119%	1.7523%
10	0.9969	0.9968	0.9968	0.9968	0.9969	0.9968	0.3156%	1.5169%
SD of mean							0.0056%	

$$\tau(T) = \tau_0 e^{\frac{E_A}{kT}} \quad (1.2)$$

Here,  $T$  is the temperature (K),  $k$  is the Boltzmann constant,  $E_A$  is the activation energy, and the relaxation time  $\tau$  ( $T$ ) is obtained by the Arrhenius equation (1.2). Further,  $C$  represents a capacitance at the time of convergence,  $C_\infty$  is a steady-state capacitance,  $C_0$  is a temporary

capacitance, and  $\beta$  is a exponent. From the above equations it can be seen that capacitor aging is dependent on temperature and time.

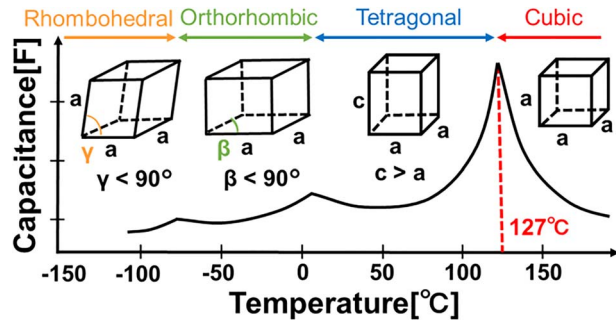
The capacitance of the capacitor using barium titanate changes according to the irradiation dose, and it was confirmed that the individual difference in capacitance change was small. However, as described above, as the total irradiation time becomes longer, the

**Table 6. Fitting parameters for aging function.**

Correct methods	Fitting area	a(C∞)	b(C0)	c(τ(t))	d(β)
Single correction	Before irradiation	0.9959	0.0041	71.9725	0.7833
	After irradiation	0.9959	0.0041	71.9725	0.7833
Step correction (12.5Gy x 4)	After 1st irradiation	0.9979	0.0045	88.5061	0.6700
	After 2nd irradiation	0.9979	0.0044	88.3359	0.6077
	After 3rd irradiation	0.9980	0.0035	93.1966	0.5558
	After 4th irradiation	0.9977	0.0038	94.3630	0.5229

**Table 7. The slope of aging-corrected capacitance change between irradiation.**

Number of fraction	Slope (x10 <sup>-7</sup> ) [sec <sup>-1</sup> ]					Average (2-5)
	1	2	3	4	5	
Single correction	-0.1942	-3.6566	-3.5211	-2.5707	-2.4514	-3.0499
Step correction	-0.1942	-0.0183	-0.1739	-0.30313	-0.00163	-0.1242

**Fig. 6. Temperature dependence of crystal structure.**

influence of the capacitance change due to aging becomes larger, which causes a decrease in measurement accuracy. Therefore, even if the total dose is the same as in the dose rate dependency and the verification of the influence by the fractionated irradiation, the measurement error due to the aging becomes large for the cases where the irradiation time is different. It is also expected that the function of subsequent aging will change with each irradiation, as both irradiation and aging reduce the capacitance. It is therefore difficult to use as a dosimeter if it is not possible to make an aging correction.

Figure 7 (a) shows the capacitance change including aging when irradiation is performed at 12.5 Gy × 4 fractions. As mentioned above, the aging is a function depending on time, and changes like the gray line in Fig. 7(a) in case without irradiation. However, as summarized in Table 6, fitting parameters for aging function varies due to irradiation. Therefore, as shown in Fig. 8(a), the functions of aging before irradiation ( $f_0(t)$ ) and aging after irradiation ( $f_1(t)$ ) are different. Furthermore, as can be seen from Table 6, as the number of irradiations increases, the difference between the function of aging before and after irradiation increases. So when fractionated irradiation is performed, it is difficult to correct the entire aging function using only the aging curve before irradiation ( $f_0(t)$ ) (Single correction, Fig. 7(b)).

Therefore, in fractionated irradiation, as shown in Fig. 8(b) and Fig. 8(c), a method was devised to correct the aging for each fraction by obtaining an aging function for each fraction after (Step correction). Figure 7(b) also shows the capacitance change after aging correction for each irradiation. In addition, Table 7 shows the slope of aging-corrected capacitance change between irradiation for each correction method. From Fig. 7(b) and Table 7, the aging correction by Step correction is much smaller in the second and subsequent irradiations compared to the single correction. The average value for the second to fifth irradiations was  $-3.0499 \times 10^{-7}$  [sec<sup>-1</sup>], whereas the step correction was  $-0.1242 \times 10^{-7}$  [sec<sup>-1</sup>].

Figure 9 (a) and (b) shows capacitance change before and after correction of the dose rate (Table 2) and the irradiation pattern (Table 3). The standard deviations of the mean due to the dose rate and the irradiation pattern were reduced from 0.0359% to 0.0057% and from 0.0732% to 0.0086%, respectively. Furthermore, under the same conditions as the experimental geometry described above, a dose from 0 to 100 Gy was irradiated every 10 Gy to create a conversion function from capacitance change to absorbed dose (Fig. 10(a)). Figure 10(b) shows that relation between irradiated dose and measured dose converted from capacitance change. As shown in Fig. 10(b), since the measured dose is agreed with the irradiation dose, barium titanate capacitor can be considered to be sufficiently usable as a dosimeter [12]. We confirmed that the correction of aging reduced the measurement error. However, in this research only verification by 6 MV-X-rays was performed. The contribution of the scattered radiation becomes large when irradiated with low energy. In future research, it is therefore necessary to use irradiation devices with different energies to verify the energy dependence.

## CONCLUSION

Multilayer ceramic capacitors using barium titanate are widely applicable as a novel dosimeter because of their low cost and small size. In addition, since the capacitance is recovered by the annealing process,

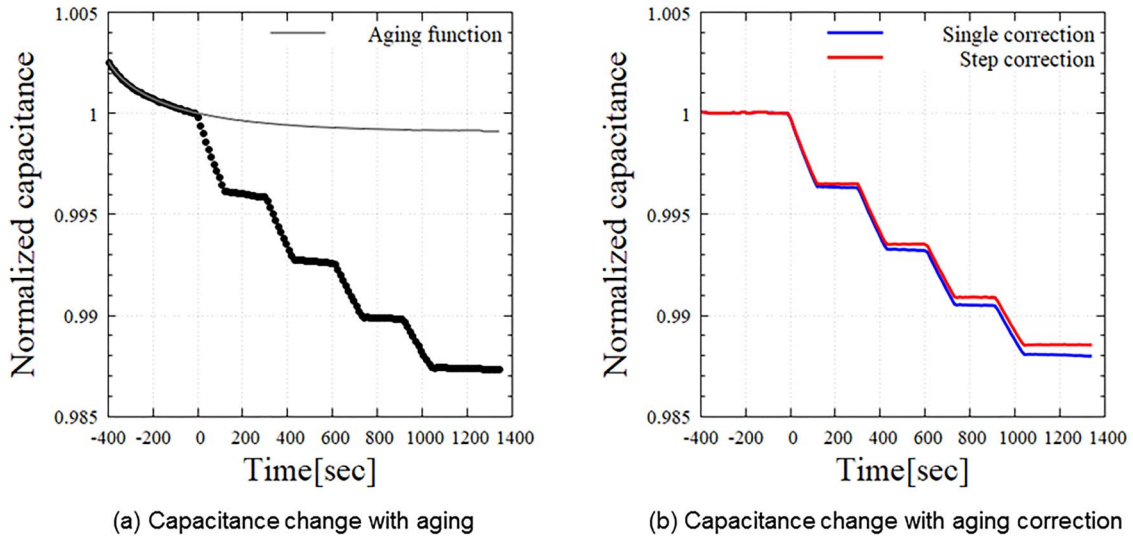


Fig. 7. Measurement data before and after correction.

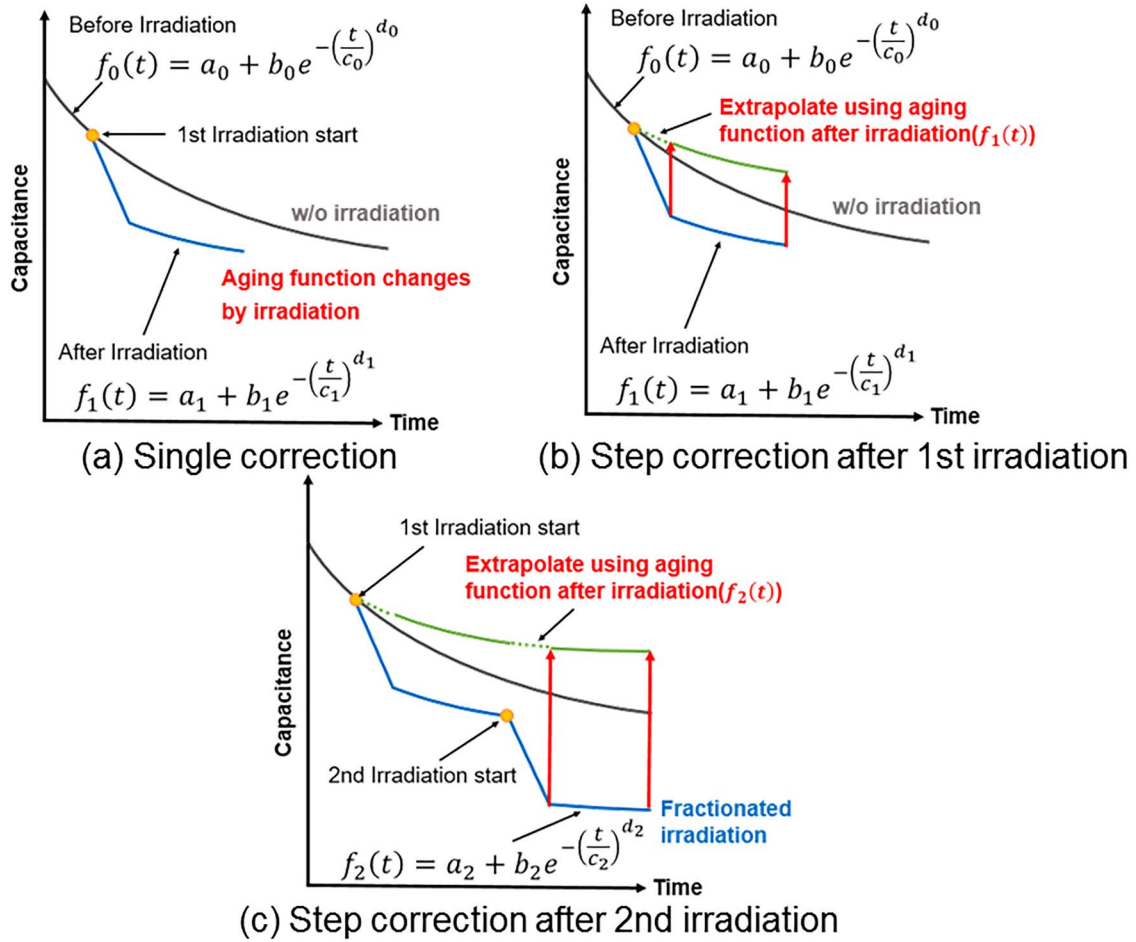


Fig. 8. Correction method of aging considering each irradiation.



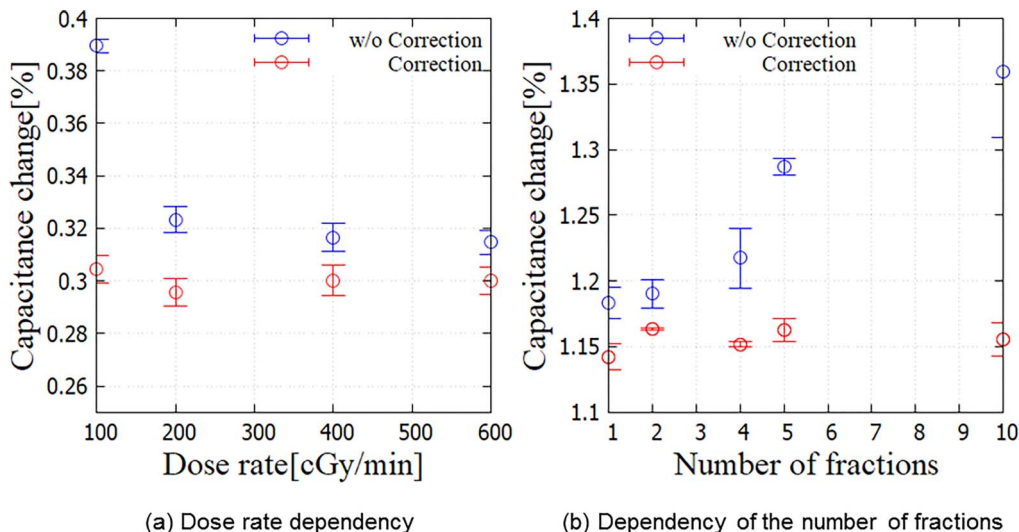


Fig. 9. Capacitance change w/and w/o correction for the dose rate dependency and the dependency of the number of irradiations.

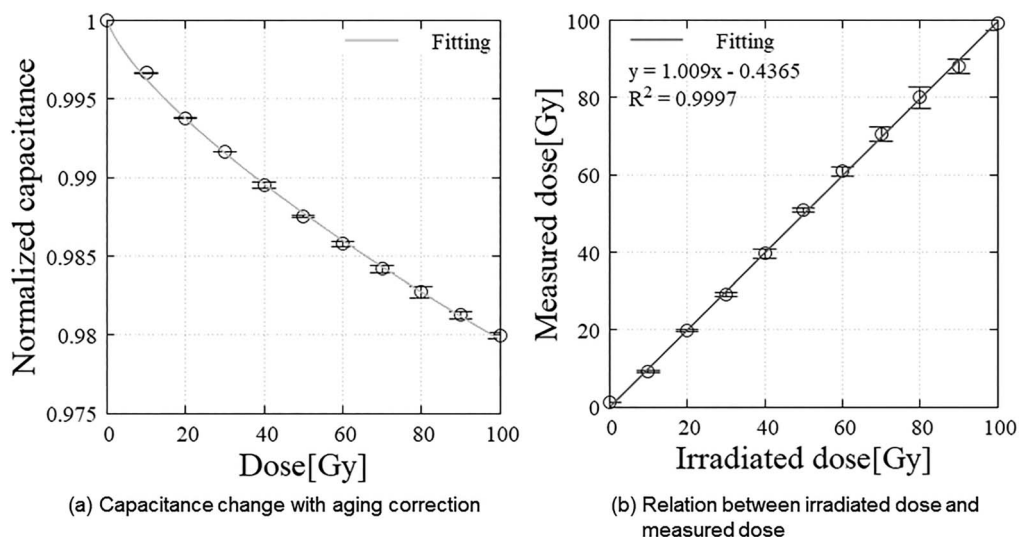


Fig. 10. Capacitance change with correction and relation between irradiated dose and measured dose.

it can be repeatedly used as a dosimeter. The present study shows that by arranging the capacitors in an array, it is possible to realize a two-dimensional detector used for QA of radiation therapy with high spatial resolution and low cost. Furthermore, the barium titanate capacitor can also be applicable as an *in-vivo* dosimeter because of its small size.

**CONFLICT OF INTEREST**

There is no conflict of interest to be disclosed.

**FUNDING**

This study is supported in part by JSPS KAKENHI (Grant No. 24659552).

**PRESENTATION AT A CONFERENCE**

Not presented.

**REFERENCES**

1. Zelefsky MJ, Fuks Z, Happersett L et al. Clinical experience with intensity modulated radiation therapy (IMRT) in prostate cancer. *Radiother Oncol* 2000;55:241–9.
2. Kutcher G, Stern R, Fraass B et al. American Association of Physicists in Medicine radiation therapy committee task group 53: Quality assurance for clinical radiotherapy treatment planning. *Med Phys* 2002;25:1773–829.
3. Kantz S, Troeller Mcdermott A, Söhn M et al. Practical implications for the quality assurance of modulated radiation therapy

- techniques using point detector arrays. *J Appl Clin Med Phys* 2017;18:20–31.
4. Borca VC, Pasquino M, Russo G et al. Dosimetric characterization and use of GAFCHROMIC EBT3 film for IMRT dose verification. *J Appl Clin Med Phys* 2013;14:158–71.
  5. Da Rocha MSF, Pontuschka WM, Blak AR. Radiation induced capacitance in barium aluminoborate glasses. *J Non Cryst Solids* 2003;321:29–36.
  6. Srinivasan VSS, Pandya A. Dosimetry aspects of hafnium oxide metal-oxide-semiconductor (MOS) capacitor. *Thin Solid Films* 2011;520:574–7.
  7. Li Y, Porter WM, Ma R et al. Capacitance-based Dosimetry of co-60 radiation using fully-depleted silicon-on-insulator devices. *IEEE Trans Nucl Sci* 2015;62:3012–9.
  8. Yuh J, Nino JC, Sigmund WM. Synthesis of barium titanate (BaTiO<sub>3</sub>) nanofibers via electrospinning. *Mater Lett* 2005;59:3645–7.
  9. Trachenko K, Pruneda M, Artacho E et al. Radiation damage effects in the perovskite CaTiO<sub>3</sub> and resistance of materials to amorphization. *Phys Rev B - Condens Matter Mater Phys* 2004;70:1–6.
  10. Fang T-T, Hsieh H-L, Shiau F-S. Effects of pore morphology and grain size on the dielectric properties and tetragonal-cubic phase transition of high-purity barium Titanate. *J Am Ceram Soc* 1993;76:1205–11.
  11. Papaioannou G, Exarchos MN, Theonas V et al. Temperature study of the dielectric polarization effects of capacitive RF MEMS switches. *IEEE Trans Microw Theory Tech* 2005;53:3467–73.
  12. Lodwick CJ. Comparison of two commercial detector arrays for RapidArc quality assurance 201AD. 10:62–74.